Available online at www.sciencedirect.com
SCIENCE DIRECT®
J. Chem. Thermodynamics 37 (2005) 1219–1225
JCT
www.elsevier.com/locate/jct

Heat capacity and entropy of monoclinic Gd_2O_3

R.J.M. Konings [a,*], J.C. van Miltenburg [b], A.C.G. van Genderen [b]

[a] European Commission, Joint Research Centre, Institute for Transuranium Elements, P.O. Box 2340, D-76125 Karlsruhe, Germany
[b] Chemical Thermodynamics Group, Utrecht University, Padualaan 8, 3584 CH Utrecht, The Netherlands

Received 6 December 2004; received in revised form 24 February 2005; accepted 26 February 2005
Available online 27 April 2005

Abstract

The heat capacity of monoclinic gadolinium sesquioxide was measured by adiabatic calorimetry in the temperature range (4 to 380) K. The results are compared to published results for cubic Gd_2O_3, indicating small differences, which result in a significantly higher standard entropy at $T = 298.15$ K. The systematics in the standard entropies of the lanthanide and actinide sesquioxide series are discussed.

Keywords: Heat capacity; Standard entropy; Calorimetry; Gadolinium sesquioxide; Lanthanide sesquioxides; Actinide sesquioxides

1. Introduction

The low-temperature heat capacity of the lanthanide sesquioxides has been studied in great detail by Westrum and co-workers [1–6]. These authors reported measurements for twelve of the fifteen Ln_2O_3 compounds, four having the triclinic A-type structure (La, Ce, Pr, and Nd), one the monoclinic B-type structure (Sm) and seven the C-type cubic structure (Gd, Er, Ho, Dy, Tm, Yb, and Lu). The experimental results were carefully analysed in terms of the lattice and electronic components, the latter giving rise to Schottky anomalies for those compounds containing lanthanide ions with incompletely filled f-electron shells. The Schottky heat capacity was derived by subtracting the lattice component from the experimental results, and could be compared to the electronic heat capacity calculated from crystal field energies.

The irregular trend of the heat capacity and standard entropy of the lanthanide sesquioxides can be explained very well by this approach, and has been used by us [7] to estimate the standard entropies at $T = 298.15$ K of some actinide sesquioxides. It was assumed that the lattice entropy and heat capacity vary regularly along the sesquioxide series and can be represented by the line La_2O_3–Gd_2O_3–Lu_2O_3, $4f^0$, $4f^7$ and $4f^{14}$, respectively, in spite of the different crystal structures. This is also the case for the lanthanide trifluorides, but not for the trichlorides. This seems to be correlated to the molar volume, which shows a continuous variation in case of the trifluorides but not for the trichlorides [8]. The room temperature molar volume of the lanthanide sesquioxides is shown in figure 1. It can be seen that the variation is discontinuous between the triclinic and monoclinic polymorphs on one side and the cubic on the other. The volume difference is, however, small when compared to the lanthanide trichlorides.

In this respect, Gd_2O_3 is an very interesting compound, since the high-temperature monoclinic structure can be maintained upon cooling and exists as metastable phase at room temperature next to the cubic phase. The heat capacity of this $4f^7$ compound does not contain an electronic component, except for the very low-temperature range (<20 K), and thus represents the lattice heat capacity (and entropy). For that reason we have measured the heat capacity of monoclinic Gd_2O_3 by adiabatic

* Corresponding author. Tel.: +49 7247 951391; fax.: +49 7247 951566.
E-mail address: konings@itu.fzk.de (R.J.M. Konings).

0021-9614/$ - see front matter © 2005 Elsevier Ltd. All rights reserved.
doi:10.1016/j.jct.2005.02.014

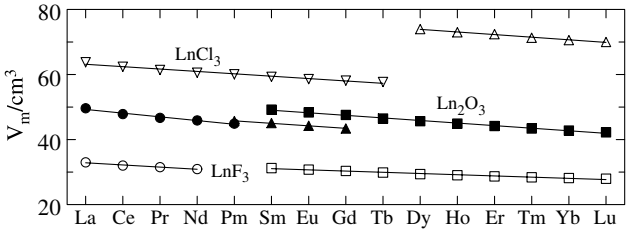

FIGURE 1. The molar volume of the different polymorphs of the lanthanide trifluorides, sesquioxides and trichlorides at $T = 298.15$ K.

calorimetry from $T = (5$ to 400) K, of which the results will be reported here. Since the heat capacity of cubic Gd_2O_3 has been measured by Justice and Westrum [2] a direct comparison of C_{lat} for the monoclinic and cubic modifications is now possible.

2. Experimental

The sample was prepared by heating of cubic Gd_2O_3 (Alfa Aesar, metal purity 0.9999) with 300 $K \cdot h^{-1}$ to $T = 1873$ K in air, at which temperature it was kept for 2 h. After cooling the sample was taken out of the furnace at $T = 473$ K, and it was stored in a controlled atmosphere. A long dwell X-ray analysis (21 h) showed that the sample is single phase monoclinic, with no reflections of the cubic phase detectable.

The heat capacity was measured by adiabatic calorimetry in the temperature range (4 to 400) K. The calorimeter CAL V and its calibration were described previously [9]. The loading of the sample was done in an inert gas glove box. The measurements were made in seven series, the first and last being made around room temperature to check reproducibility.

3. Results

The experimental results for monoclinic Gd_2O_3 are given in table 1. The measurement series are listed in chronological order and are all in good agreement in the overlapping ranges. Figure 2 shows the heat capacity as a function of the temperature. It can be seen that at the lowest temperatures the heat capacity starts to rise indicating that an anomaly is likely to occur below the detection limit of the calorimeter used.

Miller *et al.* [10] concluded from magnetic measurements that monoclinic Gd_2O_3 orders magnetically below $T = 3.9$ K. The heat capacity of monoclinic Gd_2O_3 in the temperature range (1.6 to 12.5) K has been measured by Rosenblum *et al.* [11], who found a lambda-type transition with a maximum at $T = 3.80$ K. These authors made measurements on a composite of Cu and Gd_2O_3 of which the crystallographic form was revealed in a later paper by the same group [12]. The values of monoclinic Gd_2O_3 derived from that work, after extraction of the data from the graph (for a sample with a weight fraction of 0.072 Gd_2O_3) and subtracting the heat capacity of copper, are shown in figure 3. They smoothly join the present results, except their data point for the highest temperature, at which the contribution of copper is much larger than that of Gd_2O_3.

The excess heat capacity C_{exs} is obtained by subtracting the C_{lat} from the experimental data. The latter was obtained by fitting the experimental results in the temperature range (20 to 40) K to a polynomial of the type $C_p = \alpha T^3 + \beta T^2$. Numerical integration of the excess heat capacity between $T = (0$ and 20) K gives $S_{exs} = 4.14R$. This value is in good agreement with the theoretical value $2R\ln(8) = 4.15R$, where R is the universal gas constant, and J is the statistical weight of the $^8S_{7/2}$ ground term of the $4f^7$ configuration of Gd^{3+}.

The absolute entropy of monoclinic Gd_2O_3 at $T = 20$ K can now be calculated from the excess entropy plus the lattice entropy, yielding $S^\circ(20\ K) = 36.89$ $J \cdot K^{-1} \cdot mol^{-1}$. With this value the absolute entropy at $T = 298.15$ K is calculated to be $S^\circ(298.15\ K) = (157.1 \pm 0.2)$ $J \cdot K^{-1} \cdot mol^{-1}$. The smoothed thermal functions of monoclinic Gd_2O_3 from $T = (0$ to 400) K are given in table 2.

4. Discussion

4.1. Comparison to cubic Gd_2O_3

It is extremely interesting to compare our results for monoclinic Gd_2O_3 to the data for cubic Gd_2O_3. Justice and Westrum [2] measured the heat capacity of this modification from $T = (7$ to 346) K, and Stewart *et al.* [12] from $T = (1.4$ to 18) K, the results being in acceptable agreement in the overlapping temperature range. The low-temperature results for the cubic modifications also show an anomaly below 10 K, but it does not exhibit the lambda-type shape as was observed for monoclinic Gd_2O_3. Stewart *et al.* [12] concluded from the relatively large crystal field splitting needed to reproduce the peak and from EPR measurements that the anomaly in the cubic form is not a Schottky-type transition, as suggested by Miller *et al.* [10], but is related to a magnetic ordering.

The differences in the heat capacity of the cubic and monoclinic modifications of Gd_2O_3 are relatively small. Figure 4 shows the difference C_p(monoclinic) − C_p(cubic) in the temperature region above $T = 10$ K. Between (25 and 160) K the difference is significant, the heat capacity of the monoclinic form being higher by maximum 3 $J \cdot K^{-1} \cdot mol^{-1}$. Around room temperature, where the Dulong–Petit value is approached, the heat capacity of the monoclinic form is somewhat (<1 $J \cdot K^{-1} \cdot mol^{-1}$) lower.

TABLE 1
The experimental heat capacity data for monoclinic Gd_2O_3; $R = 8.314472\ J \cdot K^{-1} \cdot mol^{-1}$

T/K	$C^\circ_{p,m}/R$	T/K	$C^\circ_{p,m}/R$	T/K	$C^\circ_{p,m}/R$	T/K	$C^\circ_{p,m}/R$
			Series I				
304.91	12.72	331.72	13.10	355.58	13.36	379.55	13.59
307.89	12.77	334.69	13.13	358.57	13.40	382.56	13.61
310.86	12.82	337.67	13.17	361.56	13.42	385.56	13.64
313.84	12.85	340.65	13.21	364.55	13.46	388.57	13.66
316.82	12.89	343.63	13.23	367.55	13.47	391.59	13.69
319.80	12.94	346.62	13.27	370.55	13.49	394.60	13.70
322.77	12.99	349.60	13.30	373.55	13.53	397.62	13.71
325.75	13.03	352.59	13.33	376.55	13.55	400.65	13.74
			Series II				
83.39	4.960	143.47	8.299	205.19	10.63	267.40	12.08
85.99	5.128	146.39	8.437	208.15	10.71	270.36	12.14
88.80	5.306	149.31	8.571	211.11	10.80	273.33	12.18
91.62	5.481	152.23	8.699	214.07	10.88	276.31	12.24
94.44	5.649	155.16	8.827	217.03	10.96	279.28	12.30
97.27	5.821	158.09	8.952	219.98	11.04	282.25	12.35
100.11	6.039	161.02	9.076	222.94	11.12	285.23	12.40
102.97	6.154	163.95	9.191	225.89	11.19	288.20	12.45
105.83	6.326	166.88	9.311	228.85	11.27	291.17	12.51
108.70	6.510	169.82	9.429	231.81	11.33	294.15	12.56
111.58	6.647	172.76	9.540	234.77	11.41	297.13	12.63
114.46	6.815	175.70	9.652	237.72	11.48	300.11	12.65
117.35	6.964	178.65	9.761	240.69	11.54	303.09	12.70
120.24	7.062	181.59	9.867	243.65	11.61	306.07	12.75
123.15	7.284	184.54	9.966	246.61	11.67	309.06	12.80
126.04	7.435	187.49	10.07	249.58	11.73	312.04	12.83
128.94	7.587	190.44	10.17	252.54	11.80	315.03	12.87
131.83	7.737	193.39	10.26	255.52	11.82	318.02	12.91
134.73	7.878	196.34	10.35	258.49	11.89	321.01	12.95
137.64	8.021	199.29	10.45	261.46	11.96	324.00	13.00
140.55	8.162	202.24	10.54	264.43	12.01	326.99	13.04
			Series III				
10.16	0.4751	15.84	0.3825	20.63	0.5424	26.02	0.8732
11.58	0.4005	16.98	0.4173	21.97	0.6110	27.33	0.9201
13.24	0.3837	18.14	0.4522	23.31	0.6795	28.50	0.9971
14.69	0.3813	19.29	0.5148	24.66	0.7649		
			Series IV				
5.34	0.5100	11.17	0.4222	18.46	0.4570	23.91	0.7060
5.84	0.7072	13.72	0.3825	19.86	0.5148	25.22	0.8022
6.65	0.8010	15.56	0.3849	21.24	0.5689		
8.48	0.5653	17.06	0.4210	22.65	0.6338		
			Series V				
26.08	0.8672	42.55	2.052	62.05	3.519	82.72	4.911
26.79	0.9081	44.25	2.190	63.89	3.648	84.63	5.039
27.99	0.9526	45.96	2.325	65.75	3.773	86.55	5.160
29.64	1.074	47.70	2.460	67.61	3.904	88.47	5.273
31.19	1.194	49.45	2.592	69.47	4.034	90.39	5.391
32.73	1.318	51.21	2.727	71.35	4.164	92.32	5.518
34.30	1.437	52.99	2.856	73.23	4.292	94.25	5.637
35.90	1.566	54.78	2.990	75.12	4.412	96.18	5.757
37.53	1.666	56.58	3.127	77.01	4.539	98.12	5.881
39.19	1.786	58.39	3.259	78.91	4.665	100.06	6.032
40.87	1.912	60.22	3.387	80.81	4.786		
			Series VI				
93.14	5.575	127.98	7.543	165.43	9.255	203.08	10.57
93.67	5.596	129.95	7.642	167.41	9.335	205.07	10.63
94.91	5.680	131.91	7.735	169.38	9.411	207.05	10.68

(*continued on next page*)

TABLE 1 (*continued*)

T/K	$C^{\circ}_{p,m}/R$	T/K	$C^{\circ}_{p,m}/R$	T/K	$C^{\circ}_{p,m}/R$	T/K	$C^{\circ}_{p,m}/R$
96.86	5.795	133.87	7.838	171.36	9.494	209.04	10.74
98.79	5.940	135.84	7.936	173.34	9.562	211.03	10.80
100.72	6.064	137.81	8.029	175.32	9.636	213.01	10.85
102.65	6.143	139.77	8.128	177.31	9.706	215.00	10.91
104.58	6.252	141.74	8.218	179.29	9.787	216.99	10.96
106.52	6.374	143.71	8.308	181.27	9.855	218.97	11.01
108.46	6.497	145.68	8.405	183.25	9.920	220.96	11.07
110.40	6.599	147.65	8.492	185.23	9.992	222.95	11.12
112.35	6.705	149.62	8.585	187.21	10.06	224.93	11.17
114.30	6.803	151.60	8.672	189.20	10.13	226.92	11.22
116.25	6.906	153.57	8.758	191.18	10.20	228.91	11.26
118.20	7.011	155.55	8.846	193.16	10.24	230.90	11.32
120.15	7.055	157.52	8.929	195.15	10.32	232.89	11.36
122.11	7.205	159.50	9.013	197.13	10.38	234.87	11.41
124.07	7.328	161.47	9.093	199.11	10.45	236.86	11.46
126.02	7.432	163.45	9.177	201.10	10.51		
				Series VII			
238.17	11.50	260.15	11.93	284.92	12.39	309.74	12.80
238.80	11.49	262.63	11.98	287.40	12.44	312.23	12.83
240.35	11.54	265.10	12.03	289.88	12.48	314.72	12.86
242.83	11.59	267.57	12.08	292.35	12.52	317.21	12.89
245.30	11.64	270.05	12.12	294.83	12.57	319.70	12.92
247.77	11.70	272.53	12.17	297.32	12.63	322.19	12.97
250.25	11.74	275.01	12.22	299.80	12.65	324.68	13.01
252.72	11.80	277.49	12.27	302.28	12.68	327.18	13.03
255.20	11.81	279.96	12.30	304.77	12.70	329.67	13.06
257.67	11.88	282.44	12.34	307.26	12.75		

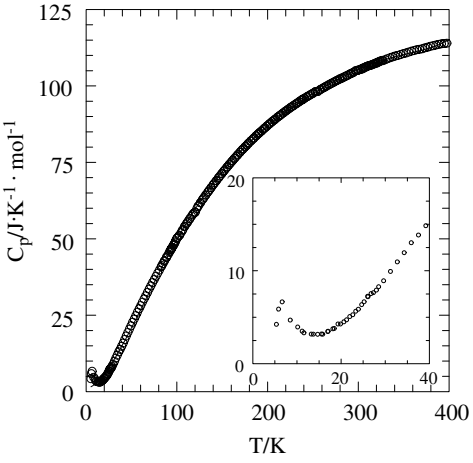

FIGURE 2. Plot of the low-temperature heat capacity of Gd_2O_3 as a function of temperature.

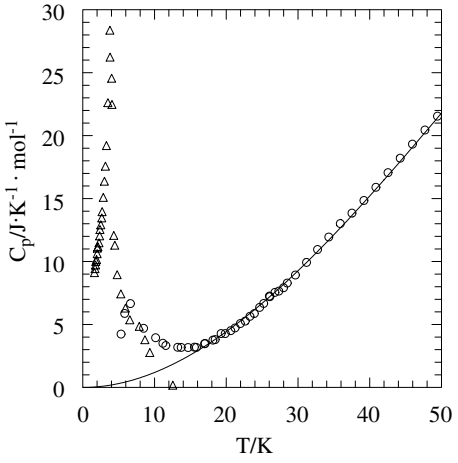

FIGURE 3. Plot of the heat capacity of Gd_2O_3 as a function of temperature; ○, present study; △, Rosenblum *et al.* [11].

As a results of the somewhat higher heat capacity at low temperature, the standard entropy of monoclinic Gd_2O_3 at room temperature is 6.5 $J \cdot K^{-1} \cdot mol^{-1}$ higher than that of cubic Gd_2O_3. This value is in very good agreement with the entropy change of the C → B transformation estimated from high pressure studies by Hoekstra [13] as 6.3 $J \cdot K^{-1} \cdot mol^{-1}$ using the Clausius–Clapeyron equation. Lutsureva *et al.* [14] derived $\Delta S = 1.26$ $J \cdot K^{-1} \cdot mol^{-1}$ from low-temperature heat capacity measurements of the monoclinic and cubic modifications of Eu_2O_3. Their results for cubic Eu_2O_3, however, appear to be too high compared to the high-temperature enthalpy data [15,16], in contrast to the results for monoclinic Eu_2O_3. A similar observation was made by Gruber *et al.* [6] for the results for Pr_2O_3 by Lutsureva *et al.* [17], and is thus likely an experimental artefact.

4.2. Comparison to monoclinic Eu_2O_3 and Sm_2O_3

Since the heat capacity of monoclinic Gd_2O_3 represents the lattice component of the monoclinic Ln_2O_3 compounds, the present results allow us to analyse the

TABLE 2
The thermodynamic functions for monoclinic Gd_2O_3 from (5 to 400) K; $R = 8.314472\ J \cdot K^{-1} \cdot mol^{-1}$

T/K	$C^\circ_{p,m}(T)/R$	$S^\circ(T)/R$	$\{H^\circ(T) - H^\circ(0\ K)\}/(R \cdot K)$
20	0.5196	4.437	4.776
25	0.7878	4.576	7.907
30	1.102	4.747	12.832
35	1.494	4.947	19.326
40	1.846	5.169	27.673
45	2.249	5.410	37.908
50	2.634	5.667	50.128
60	3.371	6.213	80.184
70	4.071	6.786	117.37
80	4.735	7.373	125.67
90	5.368	7.969	212.03
100	6.028	8.568	268.91
120	7.046	9.761	400.25
140	8.138	10.94	552.88
160	9.035	12.08	724.74
180	9.812	13.19	913.33
200	10.47	14.26	1116.3
220	11.04	15.29	1331.5
240	11.53	16.27	1557.3
260	11.92	17.21	1792.0
280	12.30	18.11	2034.4
298.15	12.64	18.89	2260.7
300	12.65	18.96	2284.2
320	12.94	19.79	2540.0
340	13.19	20.59	2800.3
360	13.41	21.34	3065.2
380	13.59	22.08	3333.9

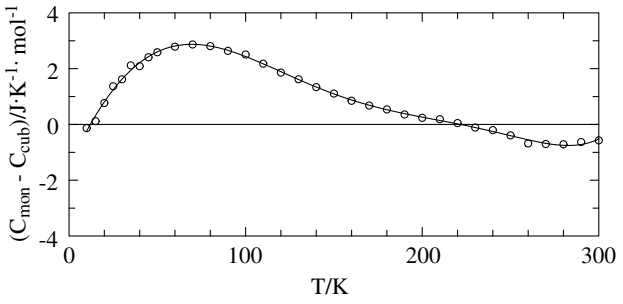

FIGURE 4. Plot of the difference between the heat capacity of monoclinic and cubic Gd_2O_3 as a function of temperature.

data for monoclinic Sm_2O_3 by Justice and Westrum [2] and monoclinic Eu_2O_3 by Lutsureva *et al.* [14] in more detail.

Justice and Westrum [2] calculated the excess heat capacity of monoclinic Sm_2O_3 by taking triclinic La_2O_3 or cubic Gd_2O_3 as lattice contribution. Both approaches revealed the Schottky anomaly in this compound, but the differences with respect to the absolute values of the excess heat capacity were significant. The excess heat capacity of Sm_2O_3 calculated with the present results for monoclinic Gd_2O_3 are shown in figure 5. This excess heat capacity in Sm_2O_3 arises from the electronic contributions of the $^6H_{5/2}$

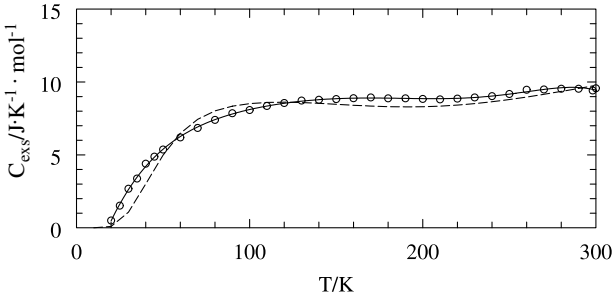

FIGURE 5. Plot of the excess heat capacity of monoclinic Sm_2O_3 as a function of temperature. The broken line shows the calculated, and the symbols the experimental result, as explained in the text.

ground state as well as the $^6H_{7/2}$ excited state, which split into, respectively, three and four doublets due to crystalline field effect. The monoclinic lanthanide sesquioxides have three inequivalent cation sites, which have the same symmetry. The crystal field levels of Sm^{3+} in the monoclinic Ln_2O_3 structure are not known for any of these sites. The excess heat capacity results obtained here have therefore been fitted by a trial and error method to a single set (0, 135, and 380) cm^{-1} for the ground state, taking the lowest doublet of the first excited state at 1020 cm^{-1}. The latter value was estimated by Borovik-Romanov and Kreines [18], and not varied.

A similar approach was applied to the data for monoclinic Eu_2O_3 by Lutsureva *et al.* [14]. In contrast to Sm_2O_3, the crystal field energies of Eu^{3+} in the monoclinic Ln_2O_3 structure are well known for all three Eu^{3+} sites from measurements of Eu^{3+} in Gd_2O_3 [19]. We have used the energies for the $^7F_0$ and $^7F_1$ states to calculate the excess heat capacity. Figure 6 shows the comparison with the excess heat capacity derived as the difference with our results for monoclinic Gd_2O_3. The calculated and 'experimental' curves have the same shape, the experimental values being somewhat higher than the calculated ones. The agreement is excellent considering that the lattice heat capacity of Eu_2O_3 is likely to be somewhat higher than that of Gd_2O_3 since it increases with increasing molar volume.

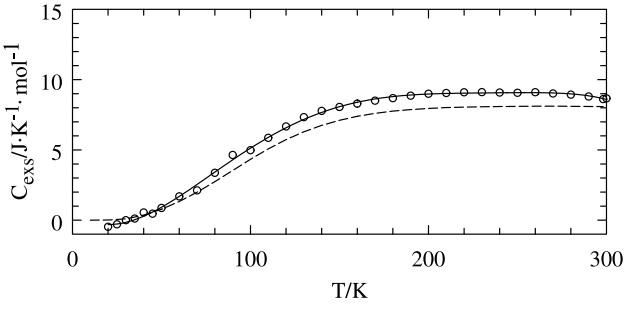

FIGURE 6. Plot of the excess heat capacity of monoclinic Eu_2O_3 as a function of temperature. The broken line shows the calculated, and the symbols the experimental results, as explained in the text.

4.3. Systematics of the Ln_2O_3 series

At room temperature, where the Dulong–Petit limit is approached, our results for monoclinic Gd_2O_3 confirm that the variation of the lattice heat capacity of the lanthanide sesquioxides can be approximated by the line La_2O_3–Gd_2O_3–Lu_2O_3. However, this is not true for the standard entropy at room temperature, because the value for S_{lat} of monoclinic Gd_2O_3 is significantly higher ($6.5\ J \cdot K^{-1} \cdot mol^{-1}$) than that of cubic Gd_2O_3. Since the molar volumes of the triclinic and monoclinic series are continuous, which can be understood from the fact that the triclinic and monoclinic structures are closely related, the transformation being displacive [20], it is likely that the lattice entropy of these Ln_2O_3 compounds can be assumed to be continuous too. The cubic structure can only be derived in a reconstructive way from the triclinic and monoclinic ones. It can thus be concluded that the lattice entropy in the Ln_2O_3 series must be described by two linear trends, as shown in figure 7. Table 3 compares the experimental entropies of the triclinic/monoclinic series and the values derived from the interpolated lattice entropy and the excess entropy calculated from the crystal field energies. This approach yield a slight but systematic overestimation of the entropies of the triclinic compounds.

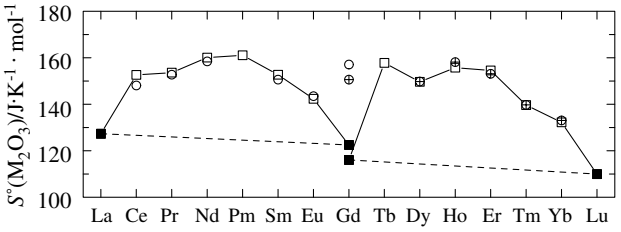

FIGURE 7. The standard entropy $S°(298.15\ K)$ of the lanthanide sesquioxides; ■, the lattice entropies derived from experimental studies; □, values calculated from the lattice the excess entropy as explained in the text; ○ and ⊕, the experimental values from the triclinic/monoclinic and cubic series, respectively.

By comparing figures 1 and 7, it becomes clear that $\Delta S_m/\Delta V_m$ is negative at the break in the lanthanide sesquioxide series, whereas this quantity is positive for break in the lanthanide trichlorides [8]. The transformation in the trichlorides corresponds, however, to a structure of lower symmetry (hexagonal to monoclinic), whereas the transformation in the sesquioxides to a structure of higher symmetry (triclinic/monoclinic to cubic).

4.4. Implications for the An_2O_3 series

The interpretation of the systematics of the heat capacity and entropy of the lanthanide sesquioxide series presented in the preceding paragraph can be considered a refinement of the one presented earlier [7], which served as a basis for estimating the standard entropies of Pu_2O_3, Am_2O_3, and Cm_2O_3. These estimates thus need small adjustments on the basis of the present results.

Pu_2O_3 and Am_2O_3 have a triclinic Ln_2O_3 structure at room temperature, Cm_2O_3 has a monoclinic structure, and correspond to the light lanthanide sesquioxides La_2O_3–Gd_2O_3(mon). Assuming, as we have done in [7], that the lattice entropy in the actinide series is parallel to that in the lanthanide series, and can be scaled on the basis of the lattice entropy derived from the experimental value for Pu_2O_3 [21], we obtain the values listed in table 3. The excess entropies for Am_2O_3 and Cm_2O_3 were simply calculated from $S_{exs} = R\ln(g_0)$. The values thus obtained are somewhat higher than our previous estimates, but well within the uncertainties.

TABLE 3
The entropies of the triclinic/monoclinic lanthanide (III) and actinide (III) sesquioxides, in $J \cdot K^{-1} \cdot mol^{-1}$

	Calculated[a]			Experimental[b]	
	S_{lat}	S_{exs}	S_{tot}	S_{exp}	Reference
La_2O_3	127.32	0.00	127.32	127.32	[1]
Ce_2O_3	126.63	11.88	150.39	148.11/148.8 ± 0.4	[5]/[22]
Pr_2O_3	125.94	13.81	150.56	152.7 ± 0.2	[c]
Nd_2O_3	125.25	17.43	160.11	158.45	[1]
Pm_2O_3	124.56	18.27	161.10		
Sm_2O_3	123.88	14.42	152.72	150.62	[2]
Eu_2O_3	123.19	9.51	142.21	143.50	[14]
Gd_2O_3	122.50	17.29	157.10	150.08 ± 0.2	This study
Pu_2O_3	134.88	14.07	163.02	163.02 ± 0.65	[21]
Am_2O_3	134.20	0.00	134.20		
Cm_2O_3	133.51	17.29	168.08		

[a] For the sesquioxides, $S_{tot} = S_{lat} + 2 \cdot S_{exs}$.
[b] The uncertainty for the standard entropies derived from the calorimetric measurements has not been given in some cases.
[c] Lutsureva *et al.* [17], as corrected by Gruber *et al.* [6].

5. Conclusion

The measurement of the low-temperature heat capacity of Gd_2O_3 has proven to be essential for the interpretation of the systematics of the lanthanide sesquioxides. This series comprises three crystallographic modifications, triclinic, monoclinic and cubic. The latter two can co-exist for Gd_2O_3 below the transition temperature. The relatively moderate difference in the heat capacity between the monoclinic and cubic modifications of Gd_2O_3, results in a significant difference in the standard entropies at $T = 298.15$ K. This difference is in agreement with the transformation entropy estimated from high pressure studies by Hoekstra [13].

Acknowledgements

The authors thank Mr. H. Hein for assistance with the sample preparation and Dr. G. Bergman (Glushko Thermocenter) for making the authors aware of the Eu_2O_3 data.

References

[1] B.H. Justice, E.F. Westrum Jr., J. Phys. Chem. 67 (1963) 339–345.
[2] B.H. Justice, E.F. Westrum Jr., J. Phys. Chem. 67 (1963) 345–351.
[3] B.H. Justice, E.F. Westrum Jr., J. Phys. Chem. 67 (1963) 659–665.
[4] B.H. Justice, E.F. Westrum Jr., E. Chang, R. Radebaugh, J. Phys. Chem. 73 (1969) 333–340.
[5] B.H. Justice, E.F. Westrum Jr., J. Phys. Chem. 73 (1969) 1959–1962.
[6] J.B. Gruber, B.H. Justice, E.F. Westrum Jr., B. Zandi, J. Chem. Thermodyn. 34 (2002) 457–473.
[7] R.J.M. Konings, J. Nucl. Mater. 295 (2001) 57–63.
[8] R.J.M. Konings, A. Kovács, in: K.A. GschneidnerJr., J.C. Bünzli, V.K. Pecharsky (Eds.), Handbook on the Physics and Chemistry of Rare Earths, vol. 33, North-Holland, Amsterdam, 2003, pp. 147–247 (Chapter 213).
[9] J.C. van Miltenburg, G.J.K. van den Berg, M.J. van Bommel, J. Chem. Thermodyn. 19 (1987) 1129–1138.
[10] A.E. Miller, F.J. Jelinek, K.A. Gschneidner Jr., B.C. Gerstein, J. Chem. Phys. 55 (1971) 2647–2648.
[11] S.S. Rosenblum, H. Sheinberg, W.A. Steyert, IEEE Trans. Mag. MAG-13 (1977) 834–835.
[12] G.R. Stewart, J.A. Barclay, W.A. Steyert, Solid State Commun. 29 (1979) 17–19.
[13] H.R. Hoekstra, Inorg. Chem. 5 (1966) 754–757.
[14] N.S. Lutsureva, G.A. Berezovskii, I.E. Paukov, Zh. Fiz. Khim. 68 (1994) 1179–1182.
[15] L.B. Pankratz, E.G. King, US Bureau of Mines, Technical Report RI-6175, 1962.
[16] D.Sh. Tsagareishvili, G.G. Gvelesiani, Russ. J. Inorg. Chem. 10 (1965) 171–172.
[17] N.S. Lutsureva, G.A. Bergaman, V.N. Naumov, G.A. Berezovsky, in: International Symposium on Calorimetry, Chemical Thermodynamics, Moscow, USSR, June, 1991, p. 52.
[18] A.S. Borovik-Romanov, N.M. Kreines, Sov. Phys. JETP 2 (1956) 657.
[19] C.A. Morrison, R.P. Leavitt, in: K.A. GschneidnerJr., L. Eyring (Eds.), Handbook on the Physics and Chemistry of Rare Earths, vol. 5, North-Holland, Amsterdam, 1982, pp. 461–692 (Chapter 46).
[20] R.G. Haire, L. Eyring, in: K.A. GschneidnerJr., L. Eyring, G.R. Choppin, G.H. Lander (Eds.), Handbook on the Physics and Chemistry of Rare Earths, vol. 18, North-Holland, Amsterdam, 1994, pp. 413–505 (Chapter 125).
[21] H.E. Flotow, M. Tetenbaum, J. Chem. Phys. 74 (1981) 5269.
[22] M.E. Huntelaar, A.S. Booij, E.H.P. Cordfunke, R.R. van der Laan, A.C.G. van Genderen, J.C. van Miltenburg, J. Chem. Thermodyn. 32 (2000) 465–482.

JCT 04-263